Chemical Enrichment in Damped Lyman α Systems From Hierarchical Galaxy Formation Models

Katsuya Okoshi, Masahiro Nagashima[1] and Naoteru Gouda

National Astronomical Observatory, Mitaka, Tokyo 181-8588, Japan;

okoshi@th.nao.ac.jp

and

Satoshi Yoshioka

Department of Physics, Tokyo University of Mercantile Marine, Tokyo 135-8533, Japan

ABSTRACT

We investigate chemical enrichment in Damped Lyman α (DLA) systems in the hierarchical structure formation scenario using a semi-analytic model of galaxy formation. The model developed by Nagashima, Totani, Gouda & Yoshii takes into account various selection effects on high-redshift galaxies and can show fundamental observational properties of galaxies, such as luminosity functions and number-magnitude/redshift relations. DLA systems offer the possibilities of measuring metal abundance more accurately than faint galaxies. For example, recent measurements of zinc abundance can provide good evidence for understanding the processes of metal pollution and star formation in DLA systems because zinc is virtually unaffected by dust depletion. Here we focus on this advantage for observation in order to explore the metallicity evolution in DLA systems at high redshifts. We can consistently show the metallicity evolution for reasonable models which also reproduce fundamental properties of local galaxy population. This result suggests that the chemical evolution of DLA systems can be consistently reconciled with the observational features of typical galaxies. We also investigate other properties of DLA systems (column density distribution and mass density of cold gas), and find that star formation in massive galaxies should be more active than that in low-mass ones. This is consistent with the results by Nagashima et al. and Cole et al. in which the star formation

[1]Present address: Department of Physics, University of Durham, South Road, Durham DH1 3LE, United Kingdam

timescale is set by reproducing cold gas mass fraction in local spiral galaxies. Finally we discuss host galaxies associated with DLA systems. We conclude that they primarily consist of sub-L^* and/or dwarf galaxies from the observations.

Subject headings: cosmology: theory - galaxies : evolution - galaxies : abundances - quasars : absorption lines

1. Introduction

The absorption-line systems observed in the spectra of background quasars have been proven to be a strong probe into the physical conditions of the Universe at high redshifts: abundances of neutral gas and metals, kinematic properties, etc. In particular, Damped Lyman α Absorption (DLA) systems, which have been associated with cold gas in proto-galactic disks (Wolfe et al. 1986), provide some advantages in the investigation of various characteristics of primordial galaxies similar to faint ones at high redshifts. For example, we can obtain abundant data in the early universe from quasar spectra which are less affected by observational limits caused by faintness of absorbers and chemical abundance, etc. Therefore, they have been studied extensively at redshifts $0 \lesssim z \lesssim 4.5$ to explore the physical processes in galaxies: star formation rates, abundances of metals and dust (Fall & Pei 1993; Lu et al. 1996; Pettini et al. 1997, 1999, 2000; Prochaska & Wolfe 1999, 2000), column density distribution (e.g. Storrie-Lombardi & Wolfe 2000; Rao & Turnshek 2000) and kinematics (Prochaska & Wolfe 1997, 1998). These observational features would provide important constraints on clarifying the evolutionary link between DLA systems and typical galaxies.

In particular, in DLA systems, we can measure abundances of various elements (Fe, Si, Ni, Mn, Cr, Zn, etc.) and thereby find good clues to the metallicity evolution of galaxies in the early universe. For example, relative elemental abundances are one of the most important complements to this information because abundance ratios of elements produced by supernovae in different proportions can provide independent insights into the chemical evolution. However, it has been difficult to establish precisely some abundance patterns (e.g. [α/Fe]) in DLA systems because the level of depletion of refractory elements onto dust grains may be uncertain. For this reason, the zinc abundance has recently been recognized as a good tracer of the metallicity evolution instead of Fe II because zinc is one of the undepleted elements. Recent observations have generally reported that the absolute Zn-abundance is $\sim 10\%$ of the solar value with no clear evolution over the redshift (Pettini et al. 1997, 1999; Prochaska & Wolfe 1999; Vladilo et al. 2000). The low abundance and the apparent lack of redshift evolution have been considered interesting problems for DLA systems as proto-

galaxies, in particular, at low redshifts where abundances much closer to the solar ones are expected. This advantage of Zn-measurement confirms that DLA systems so far remain one of the best probes at high redshifts into star formation history.

Recent theoretical studies focus on the nature of DLA systems and physical relations with galaxies observed at high and low redshifts. Katz et al. (1996) studied the formation of DLA and Lyman-limit systems in a hierarchical clustering scenario using a hydrodynamical simulations of a CDM universe($\Omega = 1$). They concluded that the observed H I column density distributions can be reproduced within a factor of 2 if DLA systems are relatively massive and dense protogalaxies. They also showed that their model could reproduce the other properties of DLA observations. However, these results remain somewhat inconclusive. The calculations were restricted to a single CDM cosmology ($\Omega = 1$ CDM). In addition, they could not include galactic disks embedded in halos with circular velocities $V_{\rm c} \lesssim 100$ km s^{-1} caused by limited resolutions ($M \sim 10^{11}\ h^{-1}\ M_{\odot}$). Gardner et al.(1997a,b, 2001) resolved these problems by using a relation between absorption cross-section σ and halo circular velocity $V_{\rm c}$ obtained from numerical simulations. Assuming that the $\sigma - V_{\rm c}$ relation can be applied for previously unresolved halos, they presented numerical results for various cosmological models. As a result, the observed abundance of DLA systems can be reproduced if their extrapolation procedure applied for less-massive halos ($V_c \gtrsim 50 - 80$ km s^{-1}). However, the validity of introducing their correction method remains uncertain. Therefore, their calculations could not still include the contribution of DLA systems below limited resolutions, especially at redshifts $0 \leq z \leq 3$. Haehnelt, Steinmetz & Rauch (1998, 2000) focussed on the kinematics to explore the nature of DLA systems in SPH simulations with high resolutions ($\sim$ a few kpc). They concluded that the high abundance of protogalactic clumps can reproduce the observed velocity width distribution and asymmetries of absorption lines found by Prochaska and Wolfe (1997,1998). Their conclusion suggested that the *majority* of DLA systems are not large, rapidly rotating disks with $V_{\rm c} \gtrsim 100$ km s^{-1} but protogalactic clumps with the typical circular velocity of DLA halos $V_{\rm c} \sim 100$ km s^{-1}. Their numerical simulations presented that their models can reproduce observational properties of DLA systems and provided interesting insights to explore the nature of DLA systems.

Recently a different approach, semi-analytic modelling, has been applied with a view to deciphering the clues to the formation process of galaxies in the hierarchical clustering scenario (e.g., Kauffmann, White, & Guiderdoni 1993; Cole et al. 1994, 2000; Somerville & Primack 1999; Nagashima, Gouda & Sugiura 1999; Nagashima et al. 2001, hereafter NTGY; Nagashima et al. 2002). These approaches have some advantages. For example, semi-analytic modelling can study the effect of star formation or supernovae feedback on galaxy evolution even under simple recipes. It does not also suffer from resolution limitations. This approach can also take into account merging the histories of dark halos based

on the power spectrum of the initial density fluctuation, and have successfully provided galaxy formation models for reproducing observational properties of galaxies such as luminosity functions, the Tully-Fisher relation, the relation between H I gas mass fraction and luminosities, and so forth. To understand the galaxy formation process, it is also important to focus on observational features of high redshift galaxies. For example, the faint galaxy number counts are good evidence for constraining the key process of galaxy formation in addition to the local feature. NTGY confirms, using a similar semi-analytic model, that the fundamental properties of local galaxies can be reproduced by their semi-analytic galaxy formation model in a cosmological constant-dominated flat universe (ΛCDM model). Their model shows good agreement with the observational features containing those of galaxies at high redshifts such as galaxy counts, taking into account high-redshift selection effects caused by cosmological dimming of surface brightness, absorption by intergalactic H I gas, and internal dust absorption. Therefore, it is valuable to examine how improvements in the above model affect our predictions for the metallicity evolution of cold gas in high-redshift galaxies. We investigate here the star formation history of DLA systems in our semi-analytic model, and whether we can consistently reproduce the metallicity evolution for the models which best match the observational constraints on local galaxy population. We also address what kinds of physical process, such as star formation timescale, play key roles in the evolution of DLA systems within the framework of the semi-analytic approach investigated here. Furthermore, we study other properties of DLA systems: H I column density distribution, mass density of cold gas and so on. Finally we discuss what kinds of galaxies are associated with DLA systems.

In §2, we briefly describe the semi-analytic model used here. In §3, we show the evolution in chemical enrichment of DLA systems. In §4, we present other properties of DLA systems in our calculation. Host galaxies of DLA systems are also discussed in this section. Finally we summarize our conclusions in §5.

2. Model

We use the semi-analytic model for galaxy formation based upon the work in NTGY. As shown in NTGY, our model reproduces luminosity functions, cold gas mass fraction, and disk radius of galaxies in the local universe and the faint galaxy number counts in the ΛCDM model.

For cosmological parameters, we adopt $\Omega_0 = 0.3$, $\Omega_\Lambda = 0.7$, $\Omega_{\rm b} = 0.015h^{-2}$, $h = 0.7$ (where h is the Hubble parameter, $h = H_0/100{\rm km\ s^{-1}\ Mpc^{-1}}$), and $\sigma_8 = 1$ that is the normalization of the power spectrum of density fluctuation given by Bardeen et al. (1986).

The cosmological parameters adopted here are consistent with recent observations, e.g., WMAP (Spergel et.al. 2003) while a slightly higher $\Omega_{\rm b}$ is favoured recently. In this paper we generally follow the model examined in NTGY. In the following, we briefly describe aspects of the model.

The number density of progenitors of a dark halo as a function of their mass and redshift is given by an extended Press-Schechter model (Press & Schechter 1974; Bond et al. 1991; Bower 1991; Lacey & Cole 1993). The number of local halos follows the Press-Schechter mass function. The merging process of dark halos is given by the method developed by Somerville & Kolatt (1999) based on a Monte Carlo method. We focus on halos with circular velocity $V_{\rm circ} \geq 40$ km s^{-1} and treat systems with small $V_{\rm circ} < 40$ km s^{-1} as diffuse accretion mass.

We assume that baryonic gas consists of two phases: cold and hot. When a halo collapses, halo gas is assumed to be shock-heated to the virial temperature of the halo and distributed in a singular isothermal sphere (*hot* gas). The cold gas is defined as the gas component within a 'cooling' radius in which hot gas cools quickly. Only a 'central' galaxy in a halo accretes the cold gas. The cold gas then becomes available for star formation. The star formation process can play an important role in chemical enrichment of cold gas. The star formation rate (SFR) is assumed as

$$\dot{M}_* = \frac{M_{\rm cold}}{\tau_*}, \tag{1}$$

where M_* and $M_{\rm cold}$ are the mass in stars and cold gas, respectively, and τ_* is the timescale of star formation. Because the star formation process has large uncertainties, it is conceivable that SFR takes place in different ways. In our model, we assume two types of star formation timescale: constant star formation (CSF) and dynamical star formation (DSF)as follows,

$$\tau_* = \begin{cases} \tau_*^0 \left(\dfrac{V_{\rm circ}}{V_*}\right)^{\alpha_*} & \text{(CSF)}, \\ \tau_*^0 \left(\dfrac{V_{\rm circ}}{V_*}\right)^{\alpha_*} \left[\dfrac{\tau_{\rm dyn}(z)}{\tau_{\rm dyn}(0)}\right] & \text{(DSF)}. \end{cases} \tag{2}$$

Note that these two are correspond the constant efficiency (CE) and accelerated efficiency (AE) models, respectively, in Somerville, Primack & Faber (2001). For the CSF model, the star formation timescale is constant at all redshifts z. For the DSF model, the timescale is proportional to the dynamical time of disks, $\tau_* \propto \tau_{\rm dyn}(z)$, which becomes shorter as redshift increases. According to Cole et al. (1994, 2000) and NTGY, we also take into account the dependence of the star formation timescale on the circular velocity, $\tau_* \propto V_{\rm circ}^{\alpha_*}$. We here adopt LC and LD models in NTGY as reference models in which the star formation timescales are given by $(\tau_*^0, V_*) = (1.5{\rm Gyr}, 300$ km s$^{-1})$ for CSF and $(4{\rm Gyr}, 200$ km s$^{-1})$ for DSF, respectively. Actually these parameters are determined by matching the cold gas

mass fraction of spiral galaxies to the one observed. Therefore, these are also expected to play an important role in determining the observable characteristics of DLA systems. It should be also noted that we here explore two types of star formation timescale according to the notation defined by Somerville & Primack (1999). One is 'Durham model' in which the star formation timescale depends only on circular velocity (Cole et al. 1994) and another is 'Munich model' in which it depends only on redshift (Kauffmann, White, & Guiderdoni 1993). Thus the star formation timescale is here assumed to totally depend on the circular velocity of halos and redshifts. For chemical enrichment, we take metal yield $y = 0.038$ adopted in NTGY.

Supernova explosions also affect galaxy evolution. We follow here a recipe for the supernova feedback process formulated in NTGY: the reheating rate of cold gas by supernova explosions is assumed to be proportional to SFR,

$$\dot{M}_{\rm reheat} = \left(\frac{V_{\rm circ}}{V_{\rm hot}}\right)^{-\alpha_{\rm hot}} \dot{M}_*, \tag{3}$$

where the values of parameters $V_{\rm hot} = 280$ km s^{-1} and $\alpha_{\rm hot} = 2.5$ are required by reproducing the observed luminosity function of local galaxies in LC and LD models in NTGY. Note that the conclusions in the previous work show that the supernova feedback process is tightly coupled with the shape and normalization of the luminosity function of local galaxies.

When two or more halos merge, the central galaxy in the largest progenitor halo becomes the new central one. All other galaxies, called 'satellite galaxies', remain to be placed around the center. After each halo-merging, we consider the following two mechanisms for mergers of galaxies: dynamical friction and random collision. Satellite galaxies merge with the central one in the dynamical friction timescale. Between satellite galaxies, random collisions also occur in the mean free timescale. When two galaxies merge, if the mass ratio of the smaller galaxy to the larger one is larger than $f_{\rm bulge}$, a starburst occurs and all cold gas is consumed(major merger). Then all stars compose a spheroidal component. Otherwise, the smaller one is simply absorbed into the disk of the larger one with no additional star formation activity(minor merger). We summarize parameter sets adopted for LC and LD models in Table 1 (the other parameters are the same as in NTGY).

Finally we define DLA systems in our model. We simply assume that all DLA systems have gaseous disks which are face-on to us (the inclination effect will be discussed in section 4) and the radial distribution of H I column density follows an exponential profile, $N_{\rm HI}(r) = N_0 \exp(-r/r_{\rm e})$, where N_0 is the central column density of neutral gas and $r_{\rm e}$ is the effective radius of gaseous disks. We here assume the effective radius $r_{\rm e} = r_0(1+z)$ where r_0 is the radius provided by specific angular momentum conservation of cooling hot gas(Nagashima et al. 2002). According to the paper, the specific angular momentum of halos has a log-normal

distribution in terms of the so-called nondimensional spin parameter λ but with a slightly large mean and dispersion, $\bar{\lambda} = 0.06$ and $\sigma_\lambda = 0.6$. The central column density N_0 is given by $N_0 = M_{\rm cold}/(2\pi\mu m_{\rm H} r_{\rm e}^2)$, where $m_{\rm H}$ is the mass of a hydrogen atom and $\mu(= 1.3)$ is the mean molecular weight. The size of DLA systems is defined by the radius R at which $N_{\rm HI} = 10^{20}$ cm^{-2}. For each system, we take the column density averaged over radius within R.

3. Chemical Enrichment in DLA Systems

Figure 1 shows the metallicity evolution of cold gas in DLA systems. The solid line shows a result for the LC model ($\tau_*^0 = 1.5$ Gyr and $\alpha_* = -2$). We compare our results here with the data given by Prochaska & Wolfe (2000) [2] and Savaglio (2000). Savaglio (2000) evaluates the metallicities of DLA systems adopting dust correction and shows ranges of the metallicity as a function of redshifts ($0 \lesssim z \lesssim 4.5$). Our calculations show that the mean metallicity increases gradually from 1/30 of solar abundance at redshift $z \sim 3$ to a half at the present due to ongoing star formation with constant efficiency. The metallicity evolution shows good agreement with the observations in the whole range of redshifts. Thus the LC model can reproduce the metallicity evolution of DLA systems, as well as many galactic properties such as luminosity function and galaxy counts. Note that the dotted line indicating mean stellar metallicity nearly traces that of cold gas. This is because cold gas is the direct material of stars.

The efficiency of star formation plays a key role in the metallicity evolution in DLA systems. In Figure 1, we also present a result for the LD model (dashed line) in which the star formation timescale is proportional to the dynamical time of disks, *i.e.*, SFR is higher at high redshifts. The resultant curve for the LD model is very shallow (1/10 solar abundance at $z \sim 5$) because SFR is much larger at high redshifts compared to that in the LC model. Therefore this model results in somewhat over-abundance compared to the high-redshift data. We thus conclude that the star formation timescale should be nearly constant in order to obtain a good agreement with the observed data for both DLA systems and local galaxies.

Now we turn to exploring the dependence of the chemical enrichment on the star formation process around the best model to reproduce the cold gas fraction well in local spiral galaxies. Figures 2(a) and 2(b) depict the effects of changing τ_*^0 and α_*, respectively, on chemical enrichment. The metal abundance strongly depends on τ_*^0 and α_* as well as on the cold gas mass fraction of galaxies (see Figure 9 in Cole et al. (2000)). Figure 2(a) shows

[2]The observed metallicity [Fe/H] from Prochaska & Wolfe (2000) is here corrected to [Zn/H] adopting [Zn/Fe]=0.4. Here we present [Zn/H] as observational data

the dependence on τ_*^0 in the LC model. As the star formation timescale is shorter (SFR is larger), the average metallicity becomes higher through metal enrichment process. We also show the dependence on α_* on the metallicity in Figure 2(b). In the LC model with $\alpha_* = -2$, comparing to the other model with $\alpha_* = 0$ that roughly corresponds to 'quiescent model' in Somerville, Primack & Faber (2001), DLA systems have low metallicities ($\sim 1/10 Z_\odot$) at high redshifts. This is because the negative value of α_* decreases SFR in low mass galaxies, which are numerous and has generally low metallicity, and then leads them to be identified as DLA systems due to increasing gas frcation. Therefore, our results are different from those found in Somerville, Primack & Faber (2001) in which DLA systems have higher metallicities of cold gas than observational data at high redshifts. We also checked the dependences of our results on other parameters such as the SN feedback-related parameters $V_{\rm hot}$ and $\alpha_{\rm hot}$ and found that they only weakly affect metallicity evolution in the whole range of redshifts. Thus, from these figures, we find that the metallicity evolution of DLA systems can be consistently reproduced by the LC model. We will see that the LC model can also successfully reproduce the column density distribution in the next section.

Next, in Figure 2(c), we present results not only for LC but for the the standard CDM (SC) and an open CDM (OC). Astrophysical parameters for SC and OC models are normalized in the same manner as LC and LD models determined by local galaxy properties (Table 1). The baryon density parameters $\Omega_{\rm b} = 0.015 h^{-2}$ are adopted for all models. The value of σ_8 is normalized by cluster abundance for models LC and OC. Note that NTGY found that LCDM is favoured by the observed HDF galaxy counts. Figure 2(c) shows that the LC model predicts the gas metallicity in the best agreement with the observed data among these cosmological models at all redshifts. While both SC and OC models totally underpredict the observed metallicity, the LC model exhibits milder evolution at high redshifts compared to the SC model and show a good agreement with the observations. Thus, also from the metallicity evolution of DLA systems, low density universes are favoured.

4. Global Properties of DLA Systems

In this section, we focus on H I column density distribution of DLA systems because we need to confirm that gas systems selected here are DLA systems. In Figure 3, we show differential distribution $f(N_{\rm HI}, X(z)) = d^2N/dN_{\rm HI}dX$, which denotes the number per unit column density $N_{\rm HI}$ and per unit absorption distance $X(z)$ (Bahcall & Peebles 1969). The data points are taken from Storrie-Lombardi & Wolfe (2000) [3] . This result is averaged over

[3]We adjust the data points for the cosmological model(LCDM) adopted here(Table 1).

redshifts $0 \leq z \leq 5$. The solid line shows a result for the LC model. The column density distribution is entirely in good agreement with the observational data. Alternatively we also present a result for the LD model (dashed line)in Figure 3. In this case, DLA systems are totally deficient over the whole range of column density. The LD model has a shorter timescale of star formation by which cold gas turns into stars more rapidly than the LC model at high redshift. Therefore, the LD model predicts smaller number of DLA systems than the LC model. Thus, the efficiency of star formation also plays an important role in the column density distribution.

It is also interesting to investigate the inclination of galactic disk. The inclination averaged cross section is half as much for random orientations although we here assume that all disks are face on to us. This corresponds to $\theta = 60^\circ$ when a disk is viewed at an angle θ to the normal. We therefore calculate the column density distribution for viewed angles: $\theta = 0^\circ,\ 30^\circ$, and 60°. Figure 4 shows how the differential distribution depends on the inclination. We find that the slope in the distribution is a little flatter when the viewed angle becomes larger because the cross section becomes small and the averaged $N_{\rm HI}$ increases by the inclination. However, the differences between the results are over all small ($\lesssim 0.1$ dex) in the observed range of column density ($N_{\rm HI} > 10^{20.3}$ cm^{-2}). Therefore, in this paper, we assume face-on for all galaxies because of the small dependence on the inclination.

To investigate the number evolution of DLA systems, in Figure 5, we also show differential distribution at four redshifts: (a)$z = 1$, (b)$z = 2$, (c)$z = 3$, and (d)$z = 4$. The observational data are from Storrie-Lombardi & Wolfe (2000). In Figure 5(a)(open circles), we also take additional data reported by Rao & Turnshek (2000) which include a sample at low redshift $\langle z \rangle \sim 0.8$. We find that our results are generally consistent with the observations. Storrie-Lombardi & Wolfe (2000) and Rao & Turnshek (2000) also pointed out that the slope in differential distributions is more moderate at lower redshifts. This is an interesting signature to discuss concerning the formation of DLA systems. However, it is still controversial to address some statements about the redshift evolution of $f(N_{\rm HI}, X)$ systematically because the samples are not so large. While the LC model can provide a reasonable fit to observations, low $N_{\rm HI}$ systems are slightly deficient at redshift $z = 4$. Although we need more observational samples to see whether this deficient should be serious, this might require some mechanism enlarging the cross section such as galactic winds pushing gas out far away from central disks.

Previously, Maller et al. (2001) investigated radial distribution of cold gas in DLA systems at high redshifts using a semi-analytic model given by Somerville, Primack & Faber (2001). They found that a Mestel distribution can reproduce column density distributions better than single-disk models (also including exponential distribution) based on angular

momentum conservation. Although Maller et al. (2001) required number suppression of DLA systems in order to match the kinematic data, the single-disk models fail to reproduce the column density distributions because DLA systems have a short radial extent so that the cross sections are too small. Figure 3 also shows results for the same model as the LC model but for $\alpha_* = 0$(dotted line). This model roughly corresponds to one in which the radial distribution of column density is of an exponential type in Maller et al. (2001, see their Figure 4). Compared with this result, our LC model predicts that DLA systems are more abundant, especially for low $N_{\rm HI}$ systems, because the negative α_* suppressed star formation in low $V_{\rm circ}$ systems (see below Figure 8). Therefore the number density is consistently high enough to reproduce column density distributions of DLA systems even in which the radial distribution of H I column density follows an exponential profile.

Generally, in Figures 3 and 5, we conclude that the LC model in our calculation can reproduce fundamental properties of DLA systems: both the metallicity evolution and the column density distribution, so that we investigate other properties of DLA systems in the LC model as we discuss below.

Figure 6 shows the mass density in HI gas contributed by DLA systems. The observed data are given by Storrie-Lombardi & Wolfe (2000) and Rao & Turnshek (2000). Our results show that the evolution of mass density is generally similar to that calculated in observations. However, the calculated density is higher than the observed data at $z \lesssim 2.5$. As discussed above, the metallicity is generally higher at low redshifts(Figure 1). This might stem from the fact that dusty systems are abundant at the present and systematically fail to be identified as DLA systems. Therefore, the local observations only show the lower limits of mass density in cold-gas systems. Furthermore, mass density is very sensitive to the number of high-$N_{\rm HI}$ systems if the power-law index β ($f \propto N_{\rm HI}^{-\beta}$) is less than 2. At $z \lesssim 2.5$, the small-number statistics of high-$N_{\rm HI}$ systems makes assessment of the mass density more uncertain, as differences in error bars of observational data between low and high redshifts in Figure 6 show. The larger sample at $z \lesssim 2.5$ would determine the data with sufficiently small errors to permit comparison with the high-redshift data.

Figure 7 shows average mass evolution of each phase. While cold gas mass is almost constant against redshift, stellar mass increases gradually towards the present because star formation proceeds to accumulate stellar mass and the merging process continues to form massive systems. At $z \sim 1$, the stellar mass exceeds that of cold gas and finally attains 10 times of cold gas in mass at present. We also calculate mass-weighted metallicities of cold gas in both DLA systems and all galaxies. The results are shown in Figure 7. Similarly to the evolution of metal mass, the metallicity increases gradually towards the present. Futhermore, the metallicities of cold gas in both DLA systems and all galaxies are quite close each other.

This indicates the fact that the chemical enrichment in DLA systems are similar to that in all galaxies.

Finally, we focus on what kinds of systems are identified as DLA systems. Figure 8 depicts average circular velocity of DLA systems at $0 \leq z \leq 5$. Similar to the mass evolution, the average circular velocity increases towards low redshifts as merging proceeds, and typical velocities are $V_{\rm circ} \sim 60$ km s^{-1} at $z \sim 3$ and $V_{\rm circ} \sim 90$ km s^{-1} at $z \sim 0$. Figure 9 shows the distribution of circular velocity. Here we present number fraction of galaxies identified as DLA systems as a function of circular velocity at redshifts (a)$z = 0$, (b)$z = 1$, (c)$z = 3$, and (d)$z = 5$, respectively. From these results, it is apparent that the dispersion of $V_{\rm c}$-distribution increases gradually towards low redshifts, similarly to the average of circular velocity. This implies that massive DLA systems form predominantly through galaxy mergers at low redshifts. At present, a few percents ($\sim 5 - 10\%$) of DLA systems can be massive systems like our Galaxy, while gaseous disks like Milky Way rarely give rise to DLA systems at high redshifts $z \gtrsim 3$. This result indicates that DLA systems are more likely to be found in less massive halos compared with typical L^* spirals. We find that this picture is strong conflict with the classical one in which DLA systems are relatively massive galaxies like our Galaxy.

Figure 10 shows absolute luminosity evolution (in U, B, V and K bands) of median host galaxies identified as DLA systems. Similarly to stellar mass, the luminosity gradually increases with the star formation. At present, the average luminosity attains $L(B) \sim 2 \times 10^9 L_\odot(B)$ and $L(K) \sim \times 10^{10} L_\odot(K)$ comparable with dwarf galaxies. Considering the other results from our calculation, *we find that host galaxies of DLA systems primarily consist of sub-L^* and/or dwarf galaxies.* Recently, Cen et al. (2002) investigated metallicity evolution of DLA systems utilizing hydrodynamic simulation. They found that DLA systems in the simulation provide good matches to observational data concerning metallicity evolution, column density distribution, redshift evolution of the neutral gas content, and so on. Simultaneously they also stressed that DLA systems comprise a mix of various morphological types including less massive systems than present-day L^* galaxies, and show that the median DLA system typically shows absolute luminosity: $L = 0.1L^*(z = 0)$ at $z = 3$ and $L = 0.5L^*(z = 0)$ at $z = 0$. This shows good agreement with our result, and also suggests that DLA systems are primarily composed of faint galaxies. Moreover, HST and ground-based observations demonstrate the direct imaging of DLA systems at $z \lesssim 1$. The results suggest that DLA systems might have mixed types of galaxies and a number of the systems are dwarf galaxies and/or compact objects (e.g. Rao & Turnshek 1998).

So far, the nature of DLA systems still remains controversial. In principle, DLA systems have a large column density in neutral hydrogen $N_{\rm HI} \gtrsim 10^{20}$ cm^{-2} comparable to the

surface density of present-day spiral galaxies. This suggests a possibility that DLA systems arise from galactic large disks (Wolfe et al. 1986). Moreover, Prochaska and Wolfe (1997, 1998) found that absorption lines of low-ionization ionic species in DLA systems show large velocity spreads and partly asymmetric profiles. They also argued that the observed kinematics can be reproduced by massive rotating disks. Alternatively, Haehnelt, Steinmetz, & Rauch (1998) showed that the majority of DLA systems are protogalactic clumps (typical circular velocity $V_{\rm c} \sim 100$ km s^{-1}) utilizing hydrodynamic simulations within the hierarchical structure formation scenario. They also stressed that the asymmetries and large velocity spreads of absorption lines associated with DLA systems can be reproduced by complex geometry and nonequilibrium dynamics of neutral gas embedded in dark halos that are not necessarily virialized. In the present work, we focus on the virialized systems, the effects of nonequilibrium dynamics of clumps are neglected, which might be important. Then further investigations will be required to clarify the kinematics of DLA systems in detail. Besides significantly larger sample than those at present, ~ 50, should be needed to discuss the kinematic data of DLA systems statistically.

Figures 11 show the cross-sections $\sigma_{\rm DLA}$ as a function of circular velocity $V_{\rm c}$ at redshifts (a)$z = 0$, (b)1, (c)3 and (d)5. This result suggests that DLA systems have typical size ~ 10 kpc at $V_{\rm c} \sim 200$ km s^{-1}. When these relations are fitted by power-law, $\sigma_{\rm DLA} \propto V_{\rm c}^{\beta}$, we find that $\beta \sim 2-3$ for each panel and that β increases slightly as redshift decreases. This relation has been investigated in hydrodynamic simulations. For example, Garder et al. (2001) showed steep scaling $\beta \sim 1.5$ for a LCDM model. Recent SPH simulations similarly found $\beta \sim 2-3$ (Haehnelt, Steinmetz & Rauch 2000; Nagamine, Springel & Hernquist 2003). While the steepness of $\sigma_{\rm DLA} - V_{\rm c}$ relations in our model is similar to that in numerical simulations, the average cross-section in our results is smaller than the numerical ones. Such large cross-sections in simulations may arise from two reasons. First, the limited resolution prevents us from resolving DLA systems with large cross-sections because they have too small cross-sections below numerical resolutions. Practically, some simulations predicted that DLA systems have quite large disks, *e.g.* ~ 100 kpc at $V_{\rm c} \sim 200$ km s^{-1}. Second, the large cross-section can be produced by neutral gas with complex geometry or/and nonequilibrium dynamics induced by frequent merging of protogalactic clumps. It is also produced even by numerical simulation with high resolution while the average cross-section is small, ~ 17 kpc at $V_{\rm c} \sim 200$ km s^{-1} (Haehnelt, Steinmetz & Rauch 2000). Therefore, the different sizes from numerical simulations may mainly stem from neglecting the latter effect.

5. Conclusions

We investigated the metallicity evolution of DLA systems in a hierarchical galaxy formation scenario using a semi-analytic galaxy formation model given by NTGY, which has been found to show good agreement with many properties of galaxies. In the previous theoretical work, it has been claimed that the metallicity of DLA systems is too high to reproduce the observed ones (e.g. Somerville, Primack & Faber 2001). We find that, in contrast to previous work, DLA systems in our model have low metallicity, $\sim 1/10 Z_{\odot}$, consistent with observational data when we use the same model as that reproducing many observations of local and high redshift galaxies given by NTGY. This conclusion is given by setting the star formation timescale as follows: (1) nearly constant against redshift, and (2) longer timescale in lower circular velocity systems. Our results suggest $\tau_* \propto V_{\rm circ}^{\alpha_*}$ and $\alpha_* = -2$, which is entirely consistent with NTGY. The first assumption (1) leads that there is a large amount of cold gas at high redshift. The second (2) indicates that a stronger α_* dependence causes low star formation rate in low mass galaxies that contribute more to the total number of DLA system. These points mainly led to the result that DLA systems have low metallicity ($Z \sim 1/10 Z_{\odot}$) consistent with observational data.

We can also reproduce column density distributions *even* under the assumption that the radial distribution of H I column density follows the exponential profile. In addition with our results for the average circular velocities and absolute luminosities, our calculation indicates that DLA systems are primarily composed of less massive systems rather than present-day L^* galaxies. In a subsequent paper, we intend to investigate in detail host galaxies of DLA systems in our model, including comparison with observational properties of dwarf galaxies and/or the other types of galaxies.

In further analyses, the following effects might be considered: First, in our model, the metal enrichment of cold gas is tightly coupled with star formation because we assume here that the metal ejected by stars is completely mixed with cold gas and finally becomes distributed throughout the disk. However, it is preferable to consider that galactic disks generally have metallicity gradients: outer regions may be metal-poor contrary to the metal-rich inner regions (Pagel 1997; Taylor 1998). Second, the metal distribution might not be consistently diffuse. Chengalur & Kanekar (2000) pointed out that typical DLA systems have a multi-phase medium composed of cold and warm H I gas induced by the observational fact that the spin temperatures of H I 21cm transition, which correspond to the kinetic temperature, appear to be higher ($T \gtrsim 1000$K) than those typical ($T \sim 100 - 200$K) of the Milky Way or nearby spiral galaxies. Moreover, Kanekar, Ghosh, & Chengalur (2001) and Lane, Briggs, & Smette (2000) found that the large amount of neutral gas is in the warm phase in two DLA systems at low redshifts from the spectra well fitted by multi-components

with various spin temperatures. The inhomogeneous gas may arise from the wide range of metallicity in present DLA systems. Moreover, local observations show that dusty systems generally have larger abundance. In practice, dusty DLA systems systematically fail to be observed because dust in DLA systems dims background quasars. These problems are clearly issues that deserve further investigation.

In the future, the combination of accurate dust-correction using various elements and detections of more DLA systems especially at $0 \lesssim z \lesssim 1$ are expected to reveal the origin of DLA systems and the star formation history at high redshifts.

We thank M.Enoki, H.Yahagi and T.Yano for valuable discussions of this study and the referee for careful reading of this manuscript and suggestions, which improved the clarity of this presentation. MN also acknowledge support from a PPARC rolling grant for extragalactic astronomy and cosmology. This work has been supported in part by the Grant-in-Aid for Scientific Research Fund(13640249) of the Ministry of Education, Science, Sports and Culture of Japan.

REFERENCES

Bahcall, J. N., & Peebles, P. J. E. 1969, ApJ, 156, L7

Bardeen, J. M., Bond, J. R., Kaiser, N. & Szalay, A. S. 1986, ApJ, 304, 15

Bond, J. R., Cole, S., Efstathiou, G., & Kaiser, N. 1991, ApJ, 379, 440

Bower, R. 1991, MNRAS, 248, 332

Chengalur, J. N., & Kanekar, N. 2000, MNRAS, 318, 303

Cen, R., Ostriker, J. P., Prochaska, J. X., & Wolfe, A. M. 2002, astro-ph/0203524

Cole, S., Aragon-Salamanca, A., Frenk, C. S., Navarro, J. F., & Zepf, S. E. 1994, MNRAS, 271, 781

Cole, S., Lacey, C. G., Baugh, C. M., & Frenk, C. S. 2000, MNRAS, 319, 168

Fall, S. M., & Pei, Y. C. 1993, ApJ, 402,479

Gardner, J. P., Katz, N., Hernquist, L., & Weinberg, D. H. 1997a, ApJ, 484, 31

Gardner, J. P., Katz, N., Weinberg, D. H., & Hernquist,L. 1997b, ApJ, 486, 42

Gardner, J. P., Katz, N., Hernquist, L., & Weinberg, D. H. 2001, ApJ, 559, 131

Haehnelt, M. G., Steinmetz, M., & Rauch, M. 1998, ApJ, 495, 647

Haehnelt, M. G., Steinmetz, M., & Rauch, M. 2000, ApJ, 534, 594

Kanekar, N., Ghosh, T., & Chengalur, J. N. 2001, A&Ap, 373, 394

Katz, N., Weinberg, D. H., Hernquist, L., & Miralda-Escudé, J. 1996, ApJ, 457, L57

Kauffmann, G., White, S. D. M., & Guiderdoni, B., 1993, MNRAS, 264, 201

Kauffmann, G. 1996, MNRAS, 281, 475

Lacey, C. G., & Cole, S. 1993, MNRAS, 262, 272

Lane, W., Briggs, F. H., & Smette, A. 2000, ApJ, 532, 146

Lu, L., Sargent, W. L. W., Barlow, T. A., Churchill, C. W., & Vogt, S. 1996, ApJS, 107, 475

Maller, A. H., Prochaska, J. X., Somerville, R. S., & Primack, J. R. 2001, MNRAS, 326, 1475

Nagamine K., Springel, V., & Hernquist, L. 2003, astroph-0302187

Nagashima, M., Gouda, N., & Sugiura, N. 1999, MNRAS, 305, 449

Nagashima, M., Totani, T., Gouda, N., & Yoshii, Y. 2001, ApJ, 557, 505 (NTGY)

Nagashima, M., Yoshii, Y., Totani, T., & Gouda, N. 2002, ApJ, 578, 675

Pagel, B. 1997, *Chemical Evolution and Nucleosynthesis*(Cambridge: Cambridge Univ Press)

Pettini, M., Smith, L. J., King, D. L., & Hunstead, R. W. 1997, ApJ, 486, 665

Pettini, M., Ellison, S., Steidel, C. C., & Bowen, D. V. 1999, ApJ, 510, 576

Pettini, M., Ellison, S., Steidel, C. C., Shapley, A., & Bowen, D. V. 2000, ApJ, 532, 65

Press, W., & Schechter, P. 1974, ApJ, 187, 425

Prochaska, J. X., & Wolfe, A. M. 1997, ApJ, 486, 73

Prochaska, J. X., & Wolfe, A. M. 1998, ApJ, 507, 113

Prochaska, J. X., & Wolfe, A. M. 1999, ApJS, 121, 369

Prochaska, J. X., & Wolfe, A. M. 2000, ApJ, 533, L5

Rao, S. M., & Turnshek, D. A. 1998, ApJ, 500, L115

Rao, S. M., & Turnshek, D. A. 2000, ApJS, 130, 1

Savaglio, S. 2000, *The Extragalactic Infrared Background and its Cosomlogical Implicatios*, IAU Symposium, Vol.204

Somerville, R. S., & Kolatt, T. 1999, MNRAS, 305, 1

Somerville, R.S., & Primack, J. R. 1999, MNRAS, 310, 1087

Somerville, R.S., Primack, J. R., & Faber, S. M. 2001, MNRAS, 320, 504

Storrie-Lombardi, L. J., & Wolfe, A. M. 2000, ApJ, 543, 552

Spergel, D.N., Verde, L., Peris, H. V., Komatsu, E., Nolta, M. R., Bennet, C. L., Halpern, M., Hinshaw, G., Jarosik, N., Kogut, A., Limon, M., Meyer, S. S., Page, L., Tucker, G. S., Weiland, J. L., Wollack, E., & Wright, E. L. 2003, astro-ph/0302209

Taylor, J. 1998, ApJ, 497, L81

Vladilo, G., Bonifacio, P., Centurion, M., & Molaro, P. 2000, ApJ, 543, 24

White, S. D. M., & Frenk, C. S. 1991, ApJ, 379, 52

Wolfe, A. M., Turnshek, D. A., Smith, H. E., & Cohen, R. D. 1986, ApJS, 61, 249

Table 1: Model Parameters

	cosmological parameters				astrophysical parameters				
CDM Model	Ω_0	Ω_Λ	h	σ_8	$V_{\rm hot}$ (km s^{-1})	$\alpha_{\rm hot}$	τ_*^0 (Gyr)	α_*	$f_{\rm bulge}$
LC	0.3	0.7	0.7	1	280	2.5	1.5	-2	0.5
LD	0.3	0.7	0.7	1	280	2.5	4	-2	0.5
SC	1	0	0.5	0.67	320	5.5	4	-3.5	0.2
OC	0.3	0	0.6	1	220	4	1	-3	0.5

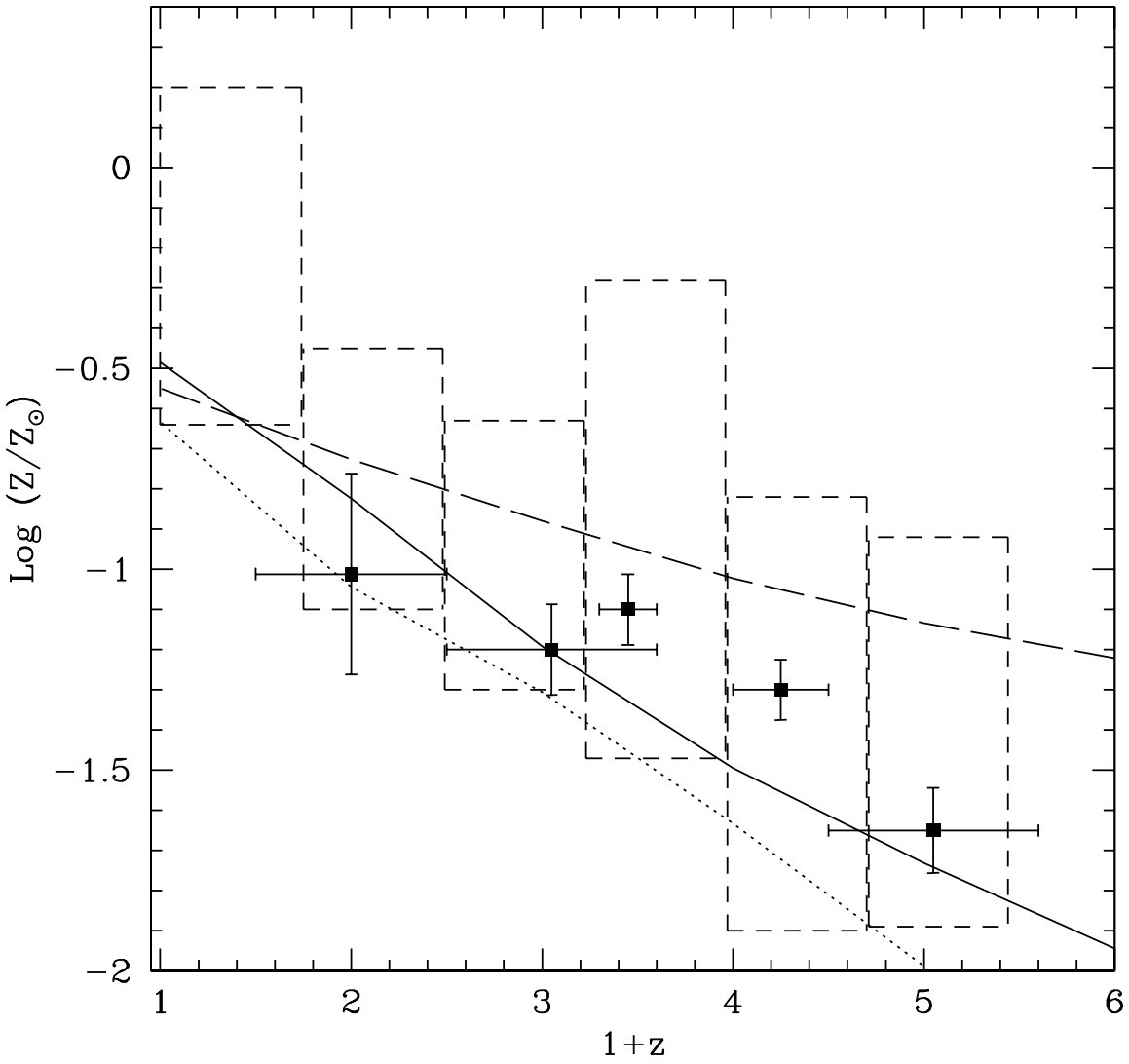

Fig. 1.— Metallicity of cold gas in DLA systems (in units of solar abundance) as a function of redshift. The square symbols are the observed metallicity in DLA systems (Prochaska and Wolfe 2000). The boxes also represent ranges of the metallicity data corrected by dust depletion (Savaglio 2000). The solid and dashed lines show the results of the LC and LD model, respectively. Also shown for the metallicity evolution of stellar components for the LC model(dotted line).

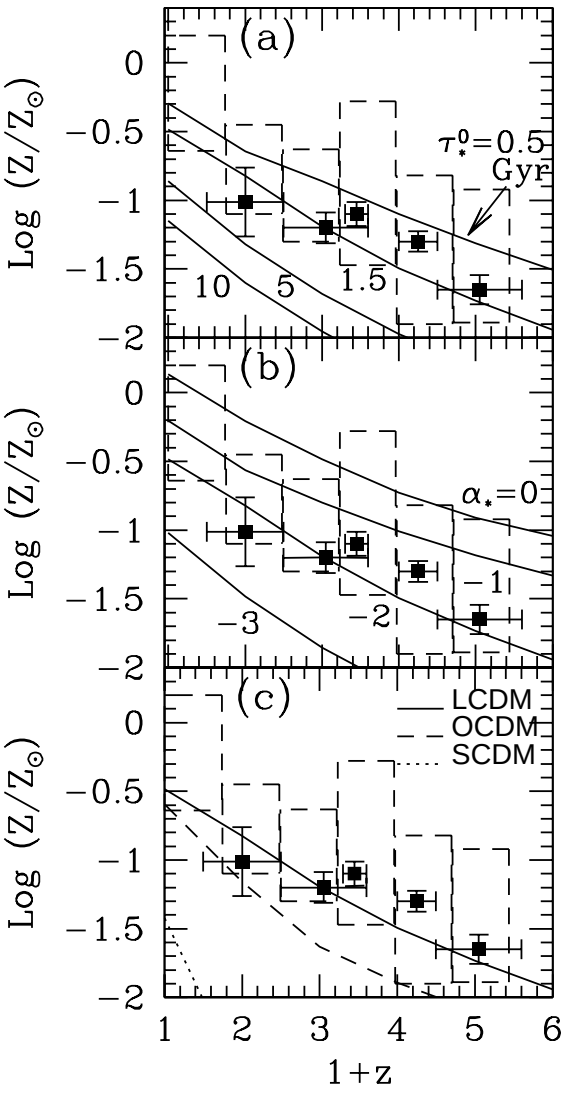

Fig. 2.— Metallicity of cold gas in DLA systems (in units of solar abundance) as a function of redshift. The observational data are also the same as in Figure 1. (a)The different lines depict the metallicity evolution for various cases of star-formation timescale: $\tau_* = 0.5,\ 1.5(Model\ LC),\ 5$ and $10\ Gyr$ from top to bottom, (b) $\alpha_* = 0,\ -1,\ -2(Model\ LC)$, and -3 from top to bottom, and (c) various cosmological models: LC(solid line), OC(dashed line), and SC(dotted line). Cosmological parameters are summarized in Table 1. All four cosmological models are taken from NTGY.

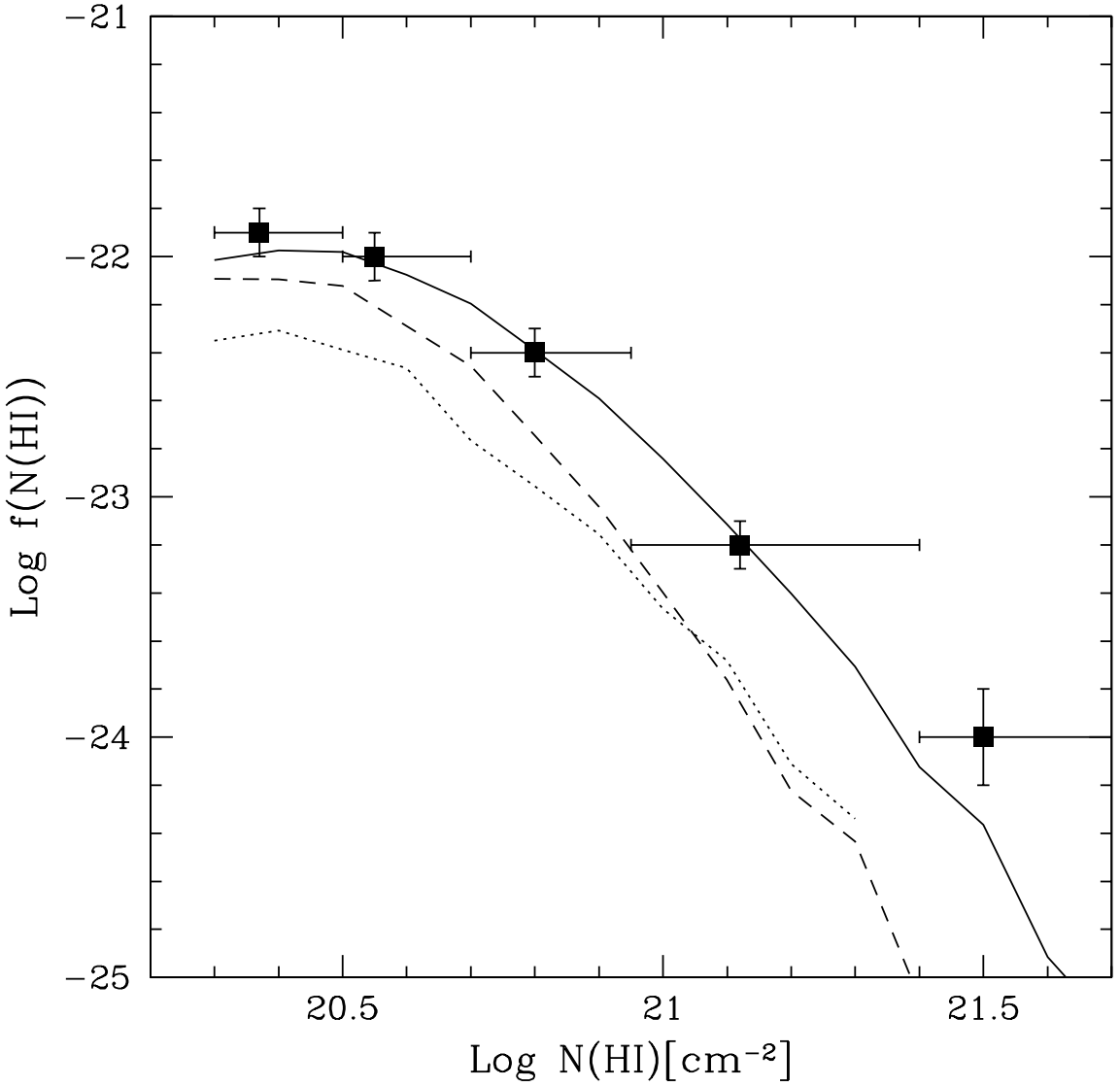

Fig. 3.— DLA column density distribution $f(N_{\rm HI})$ for three models: the LC model ($\alpha_* = -2$)(solid line), LC model except for $\alpha_* = 0$(dotted line), and LD model(dashed line). The square symbols with crosses are the observational data (Storrie-Lombardi & Wolfe 2000).

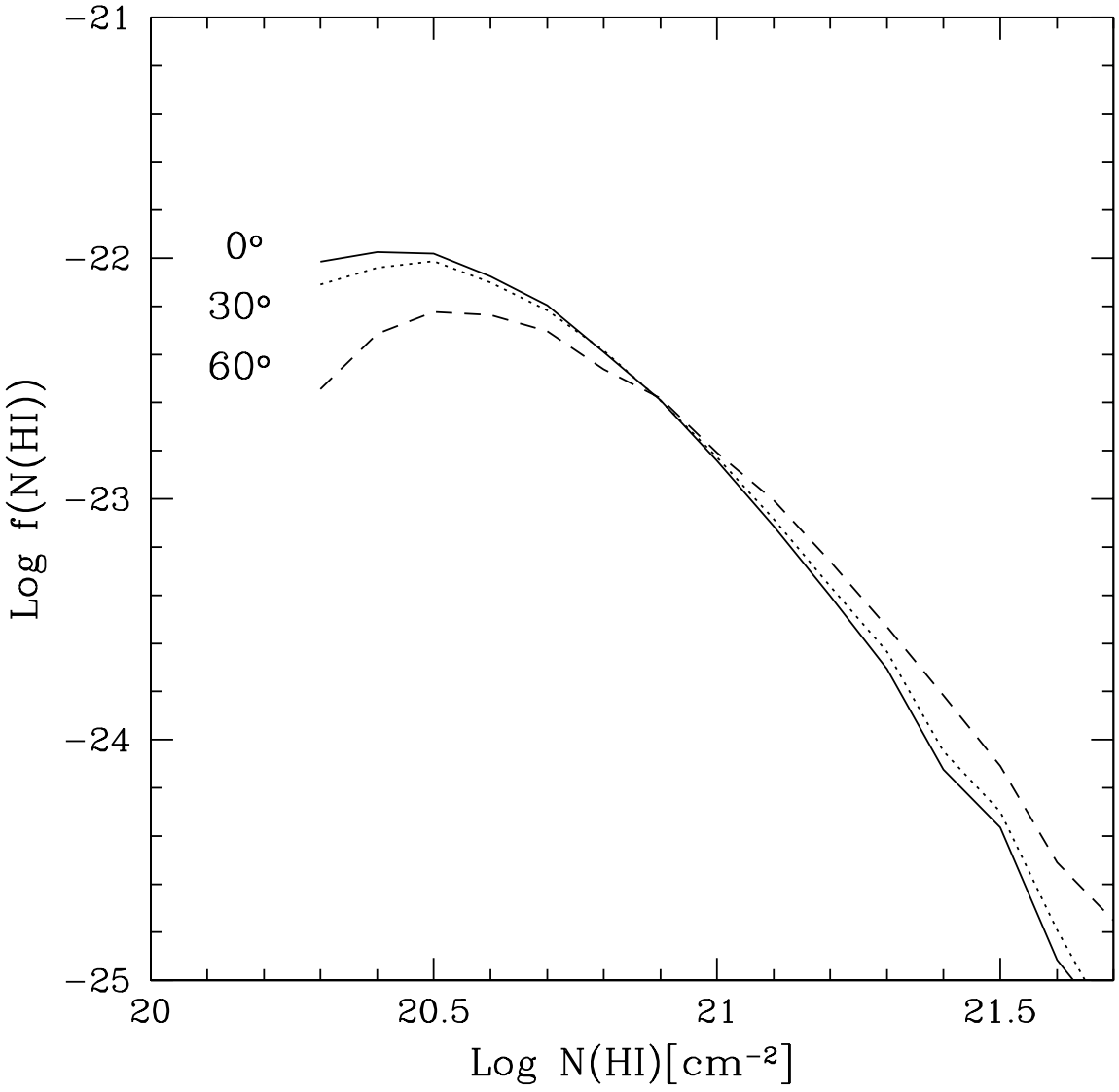

Fig. 4.— DLA column density distribution $f(N_{\rm HI})$ for three viewed-angles: $\theta = 0°$(solid line), 30°(dotted line), and 60°(dashed line).

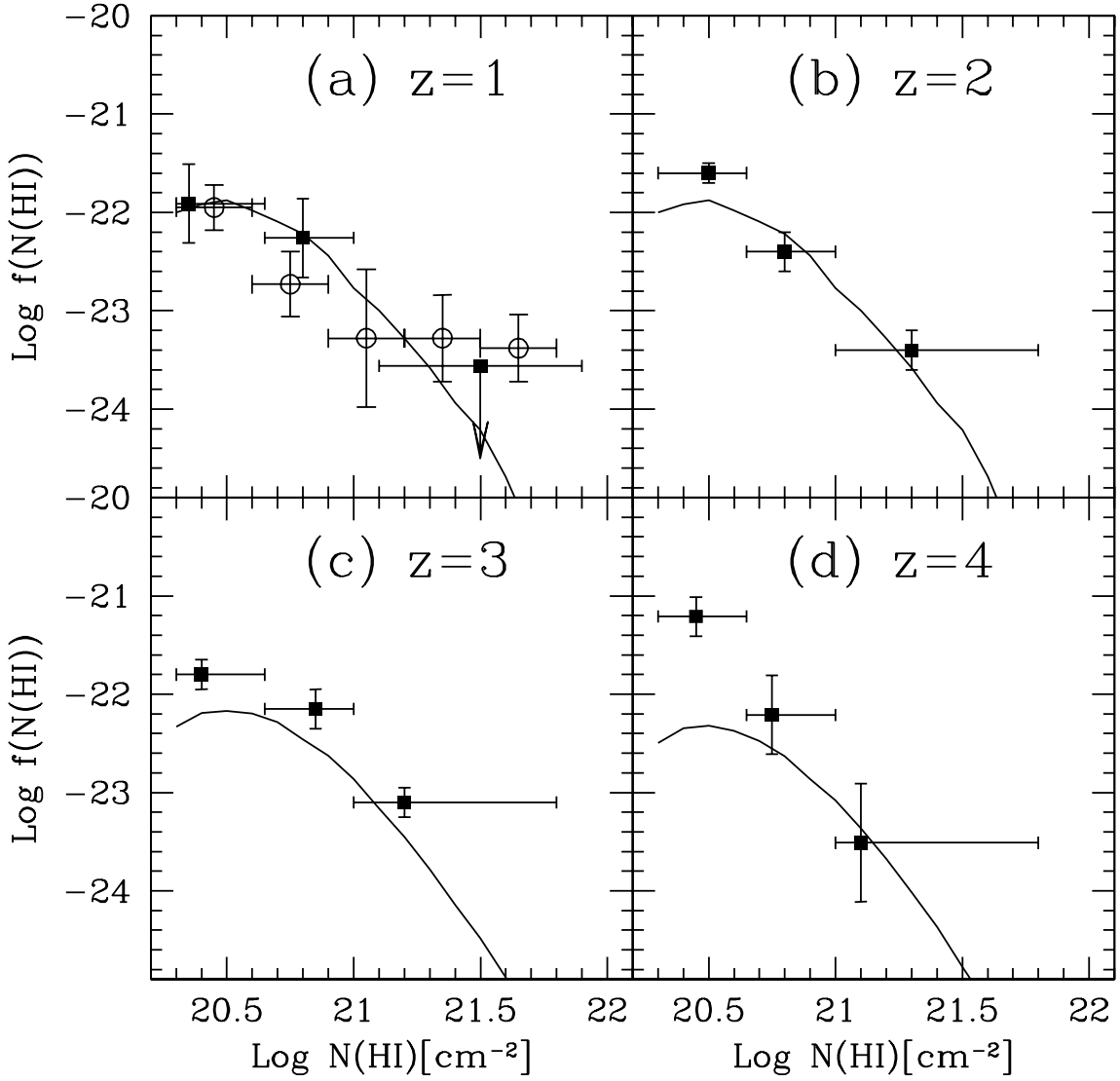

Fig. 5.— DLA column density distribution $f(N_{\rm HI})$ for the LC model at four redshifts: (a)$z = 1$, (b)$z = 2$, (a)$z = 3$, and (d)$z = 4$. The square symbols with crosses are the observed data shown in four redshifts (Storrie-Lombardi & Wolfe 2000)(closed square). Also shown in Figure (a) for another observation at $\langle z \rangle = 0.78$ (Rao & Turnshek 2000)(open circle).

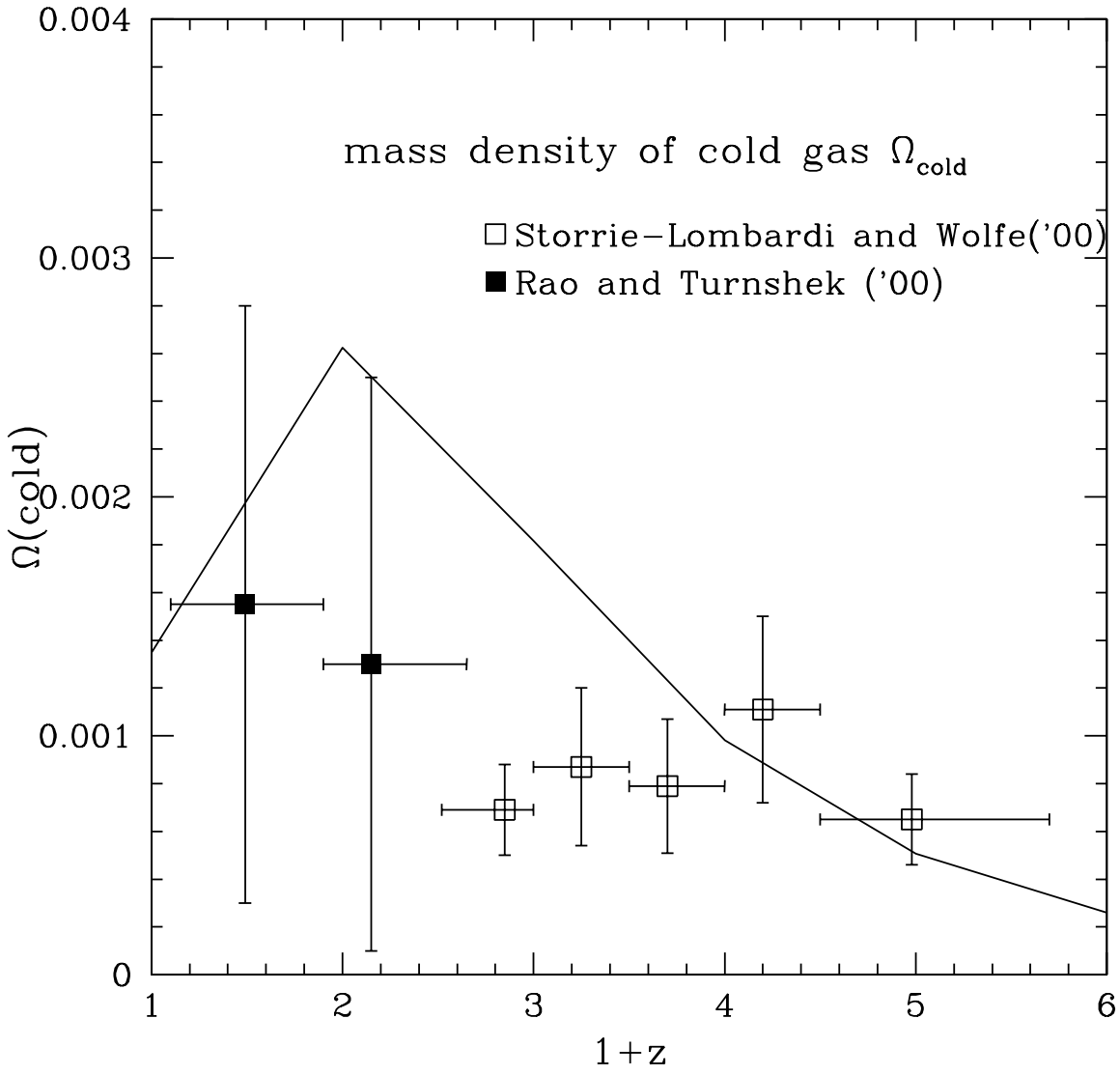

Fig. 6.— Mass density of cold gas in DLA systems as a function of redshifts. The observational data are given by Storrie-Lombardi & Wolfe (2000)(open square) and Rao & Turnshek (2000)(closed square).

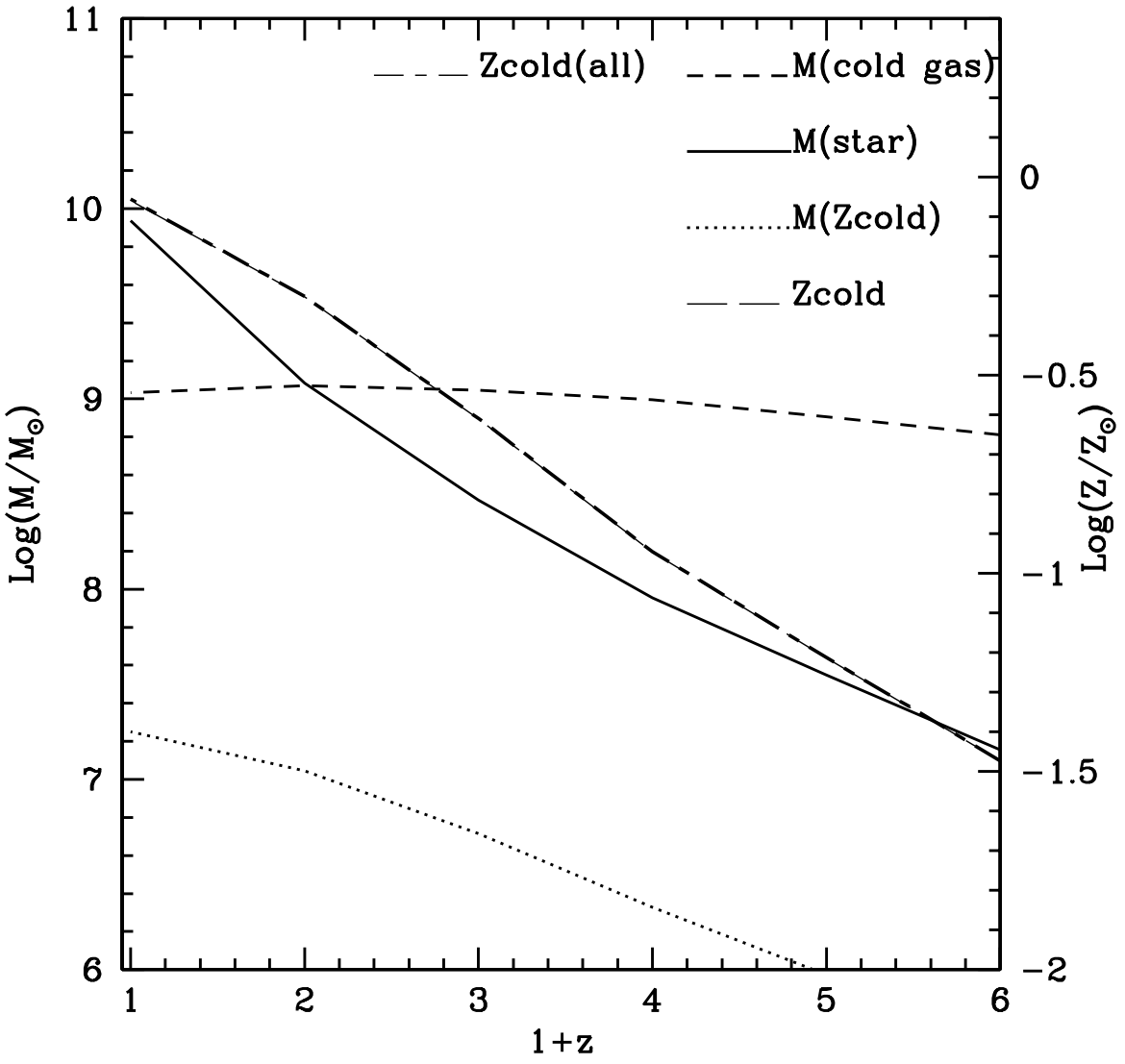

Fig. 7.— Average mass evolution of each phase as a function of redshifts: cold gas(dashed line), stars(solid line), and metals(dotted line). Metallicity weighted by mass Zcold is depicted as long-dashed line. We also show the mass-weighted metallicity of all cold gas Zcold(all) as dot-dashed line which is almost identical with Zcold(long-dashed line).

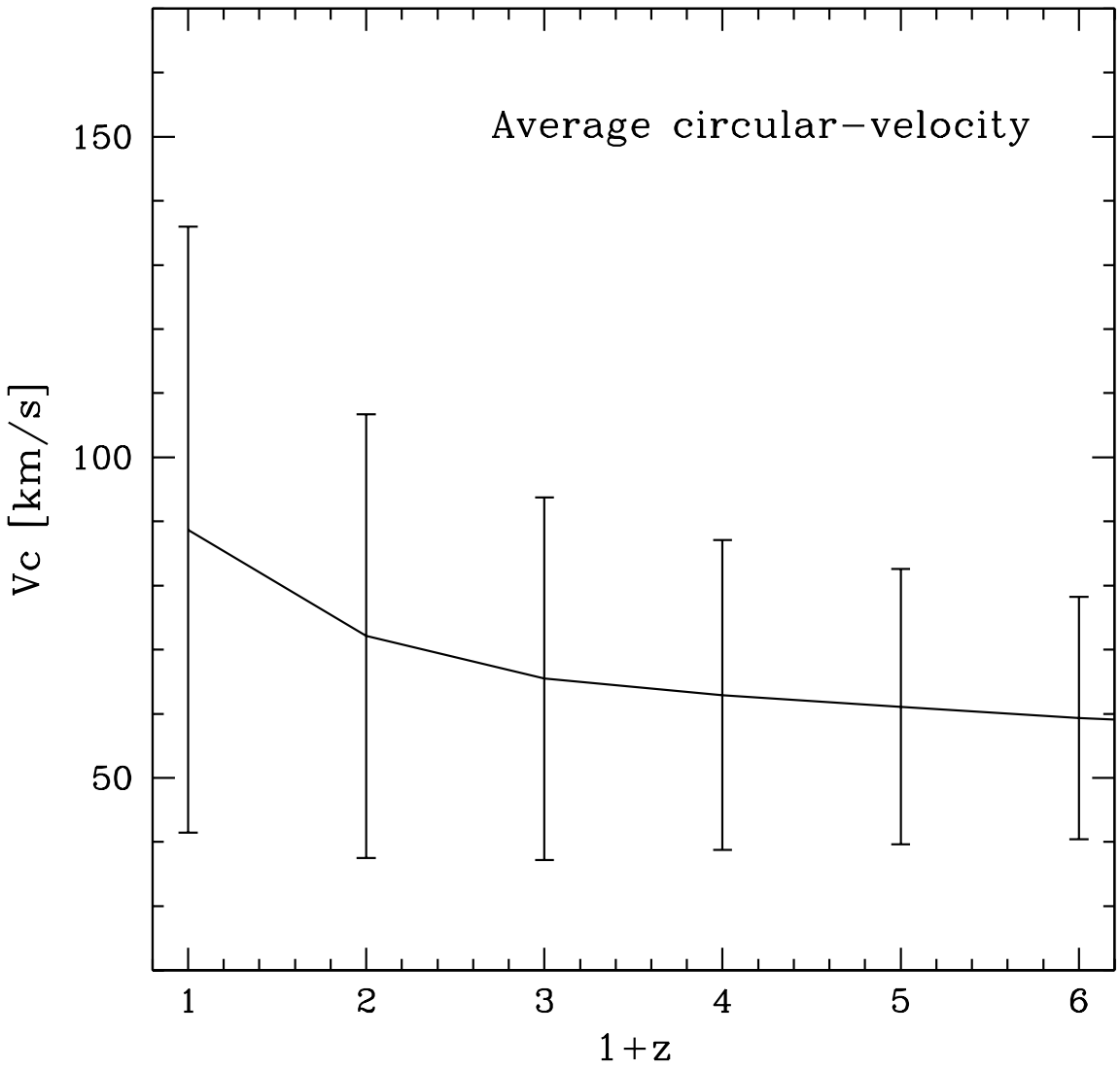

Fig. 8.— Evolution of average circular velocity $V_{\rm circ}$ of DLA systems. Error bars with the averages indicate 1σ errors.

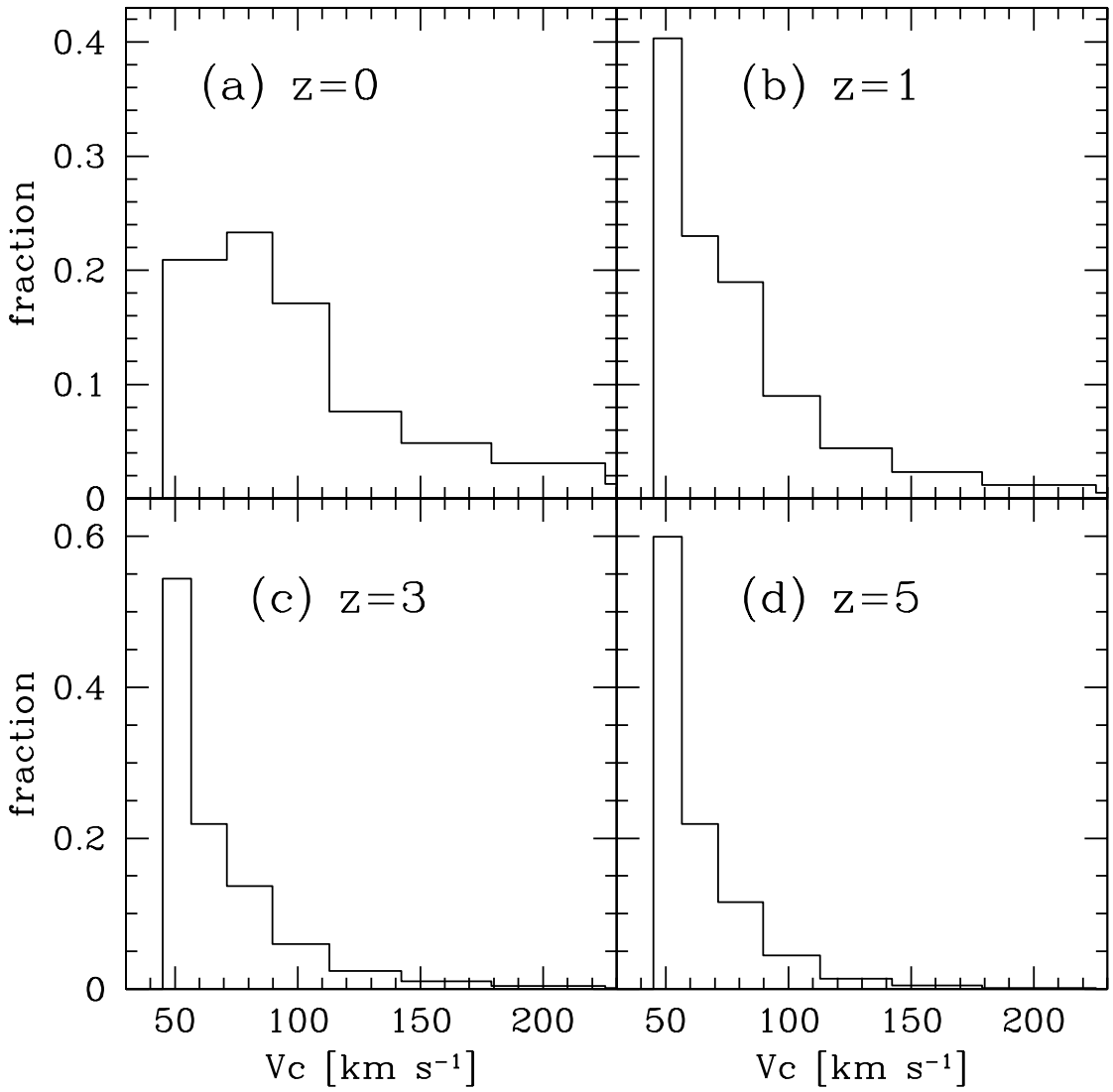

Fig. 9.— The distribution of circular velocity $V_{\rm circ}$ at four redshifts: (a)$z = 0$, (b)1, (c)3 and (d)5.

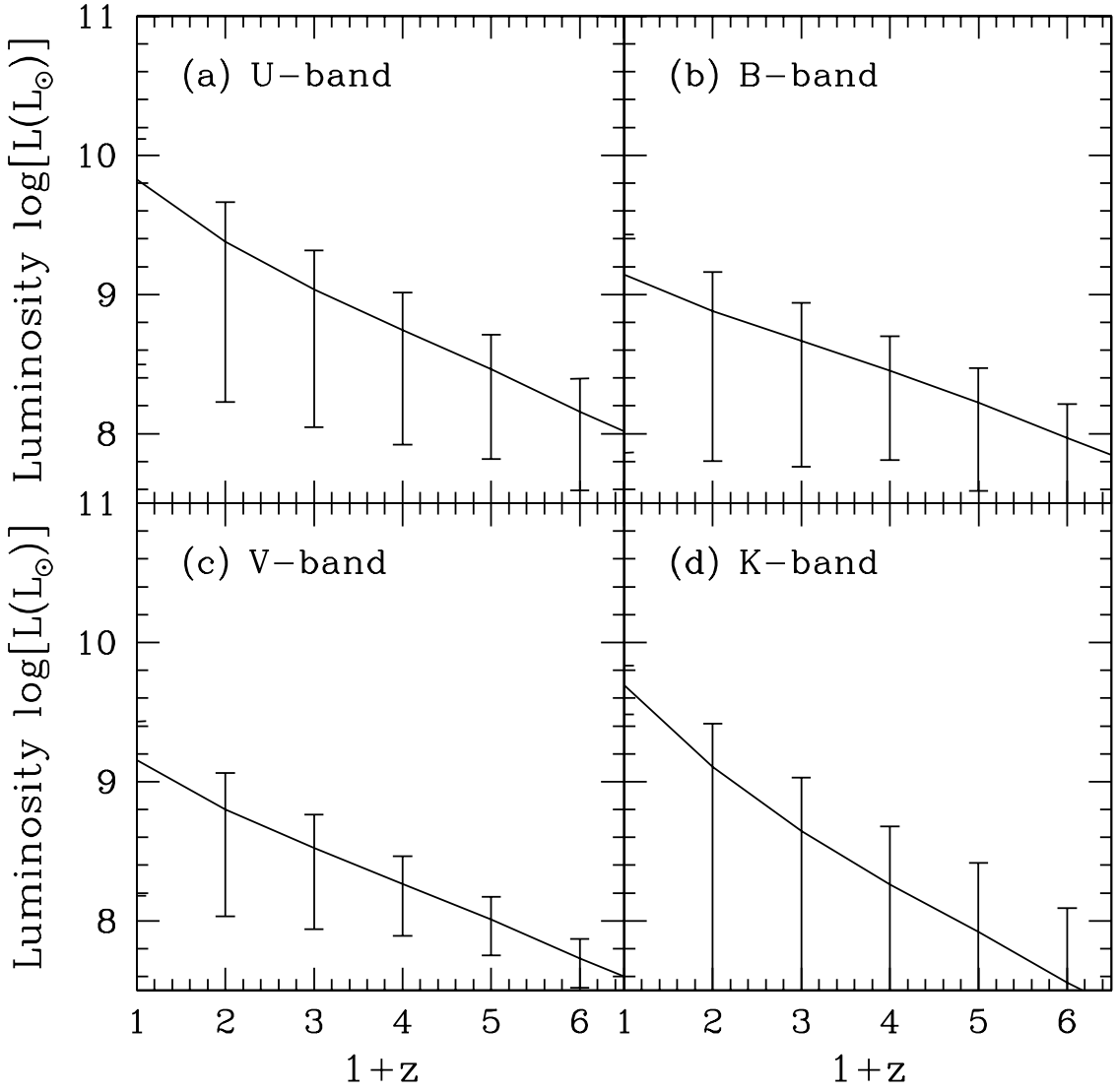

Fig. 10.— Average luminosity evolution of host galaxies identified as DLA systems in four bands: (a)U-band, (b)B-band, (c)V-band and (d)K-band. 1σ errors are shown by error bars with the averages.

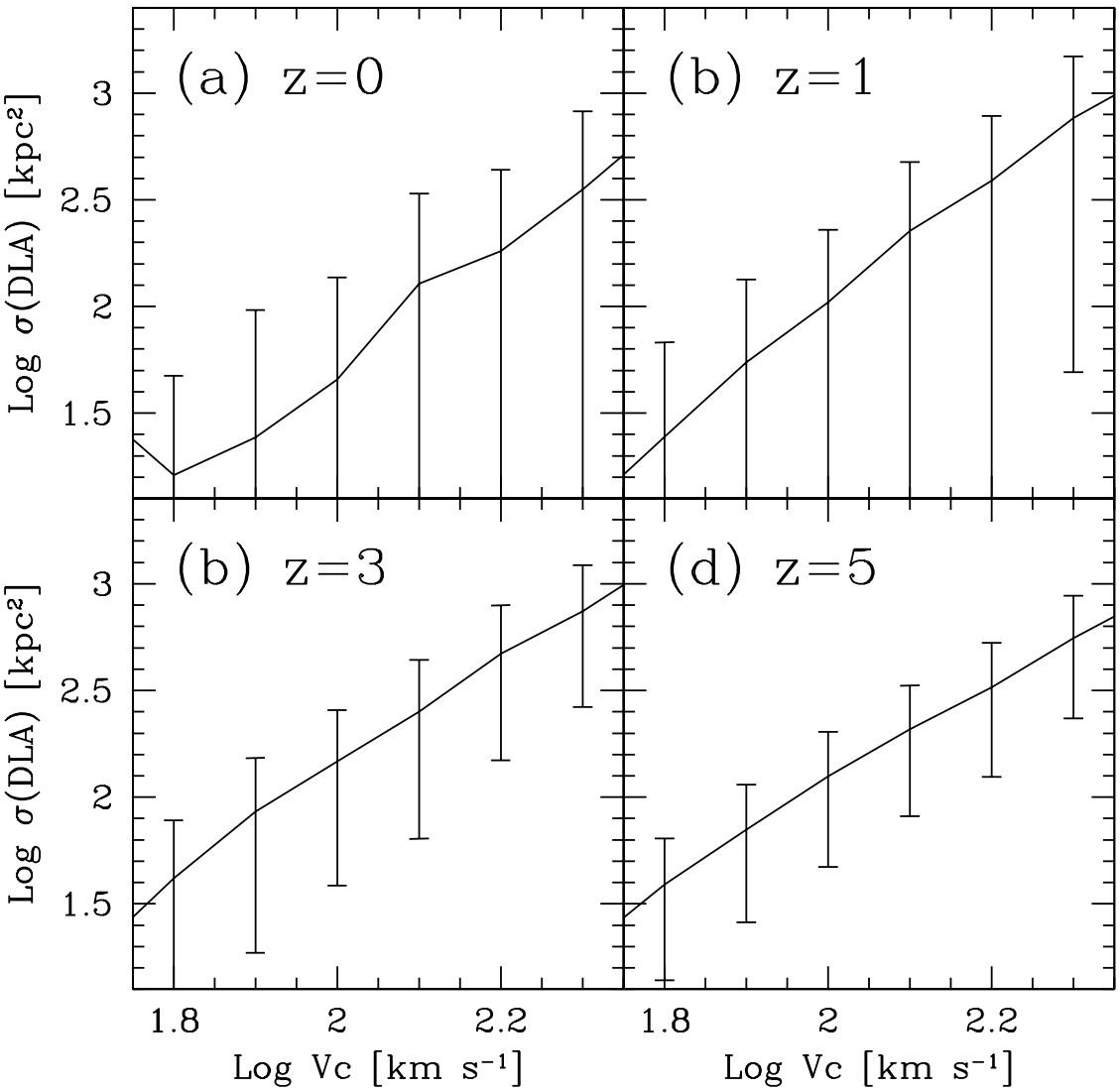

Fig. 11.— Average cross sections of DLA systems as a function of circular velocity $V_{\rm circ}$ at redshifts (a)$z = 0$, (b)1, (c)3, and (d)5. In each panel, error bars indicate 1σ errors.